

# Photoluminescence signature of silicon interstitial cluster evolution from compact to extended structures in ion-implanted silicon

P K Giri

Department of Physics, Indian Institute of Technology Guwahati, Guwahati 781039, India

Received 28 January 2005, in final form 9 March 2005

Published 3 May 2005

Online at [stacks.iop.org/SST/20/638](http://stacks.iop.org/SST/20/638)

## Abstract

Low temperature photoluminescence (PL) studies have been carried out on ion-implanted silicon in order to elucidate upon the structure evolution of the self-interstitial (I) clusters as a function of implantation dose, energy, species and post-implantation annealing conditions. PL measurements on as-implanted and low temperature annealed (up to 450 °C) Si show a sharp X band and a W band at 1200 nm and 1218 nm, respectively. The W band shows gradual quenching of PL above ~60 K with a characteristic activation energy of 59 meV. We argue that the W band originates from a compact di-interstitial cluster in Si. Short duration annealing at 600 °C results in multiple sharp peaks in the range of 1228–1400 nm for the high energy (MeV) and high dose ( $\geq 1 \times 10^{12} \text{ cm}^{-2}$ ) implantation, while low energy (keV) or low dose ions induce two broad peaks in the same wavelength range. Prolonged annealing at 600 °C induces primarily two broad peaks centred at 1322 nm and 1392 nm. These broad, but distinct, PL signatures are attributed to a chain of I-clusters, while the multiple sharp peaks possibly result from multiple configurations/ excited states of the compact but bigger I-clusters. For annealing at and above 680 °C and dose of  $\geq 1 \times 10^{13} \text{ cm}^{-2}$ , the sharp PL peak observed at 1376 nm is attributed to  $\{3\ 1\ 1\}$  rod-like defects. We argue that the changing line shape and energy of the PL spectra with processing temperature is a possible indicator of the shape evolution of the clusters from compact to extended structures as predicted recently from simulation.

## 1. Introduction

Self-interstitial defects in silicon are created through ion implantation and associated with the transient enhanced diffusion of dopants, directly [1] or indirectly through the formation of larger extended defects, such as rod-like  $\{3\ 1\ 1\}$  defects [2]. Experiments have revealed the presence of small self-interstitial clusters [3–5] prior to the formation of extended defects in Si. While the structural properties of the  $\{3\ 1\ 1\}$  defects are relatively well analysed [2, 6], and a number of theoretical models for the related I-clusters have been proposed [7–11], reliable configurations of the stable I-clusters are not fully understood. The intermediate I-clusters

that are thought to be the building blocks for extended rod-like defects are difficult to detect by conventional electric and magnetic methods. Theoretical investigations of the structure and dynamics of small I-clusters have produced a diversity of results and in most of the cases correlation with the experiment has been found to be very poor [12]. Several models including compact and non-compact structures have been proposed for di-interstitials ( $I_2$ ), tri-interstitials ( $I_3$ ) and four-interstitial ( $I_4$ ) clusters in silicon [7–11]. Recent studies have reported complexity of these small I-clusters [13]. Theoretical studies have suggested that stable interstitial (I) clusters in Si bound to dislocations may be responsible for the dislocation related photoluminescence [14]. This has opened up challenges for

a deeper understanding on the optical properties of small I-clusters.

Deep level transient spectroscopy (DLTS) and photoluminescence (PL) spectroscopy have been utilized in studying the formation and evolution of the interstitial clusters in silicon [4, 5]. Several characteristic PL peaks regarded as due to I-clusters have been reported for both n-type and p-type Si. A defect called the W centre [15], whose no-phonon peak is located at 1218 nm is commonly observed from as-implanted and low temperature annealed Si with various ions. Coomer *et al* [9] argued that a model tri-interstitial ( $I_3$ ) cluster could account for many of the fundamental properties of the W centre. However, recent first principle calculation on the vibration modes of various configurations of  $I_3$ -clusters casts considerable doubt about the identification of the W centre with the  $I_3$ -clusters [16]. On the other hand,  $I_2$ - and  $I_4$ -clusters in silicon have been identified with electron spin resonance (ESR) studies. Commer *et al* [17] proposed to attribute B3 ESR spectra, the 1039.8 meV zero phonon line (X band) in PL and infrared (IR) absorption peaks at 530 and 550  $\text{cm}^{-1}$  to the  $I_4$  defect and recent study confirms this identification [18]. The  $I_4$  defect is stable up to  $\sim 500^\circ\text{C}$ . However, the evolution of the defect spectra for annealing above  $500^\circ\text{C}$  is largely unknown. Using inverse modelling of the cluster ripening process, Cowern *et al* [19] predicted a number of intermediate size I-clusters such as  $I_4$  and  $I_8$  for small duration annealing at  $600^\circ\text{C}$  and a broad distribution of cluster sizes  $I_n$ , with  $n$  in the range of 10–200. Experimental evidence of  $I_8$ -cluster-nucleated formation of extended defects was obtained from TEM analyses [20]. However, no direct correlation exists with the simulations results on the electrical and optical signatures of the I-clusters reported so far. Recent PL studies on proton and copper implanted silicon have indicated the possible signature of intermediate size clusters [21] that form during annealing in the temperature range of  $500$ – $600^\circ\text{C}$ . Several sharp peaks and a few broad peaks have been observed between 1228 and 1400 nm for samples implanted with high energy and high dose and annealed at temperatures above  $500^\circ\text{C}$  by other groups [4, 5]. This suggests the presence of a number of stable clusters between the W and X centres and the  $\{3\ 1\ 1\}$  defects. However, no definite assignments have been made for these peaks and in some cases the assignments are found to be contradictory [4, 5]. Hence, it is necessary to investigate the nature of the defects responsible for the observed PL bands as a function of ion species, dose and energy. These studies are expected to enable better comparison with the theoretically predicted behaviour of the I-clusters.

In this work, we have investigated the photoluminescence signature of I-cluster evolution during post-implantation processing as a function of ion species, energy, dose and doping. While many studies have primarily focused on n-type silicon implanted with high energy (MeV) Si ions to enable both electrical and optical studies, this study focuses on the evolution of the PL line shape with various parameters of implantation and processing steps for p-type Si, and the results are compared with those of n-type Si. We attempt to correlate our experimental results with the theoretically predicted stability of I-clusters and their thermal evolution. It is shown that various features of the PL spectra can be

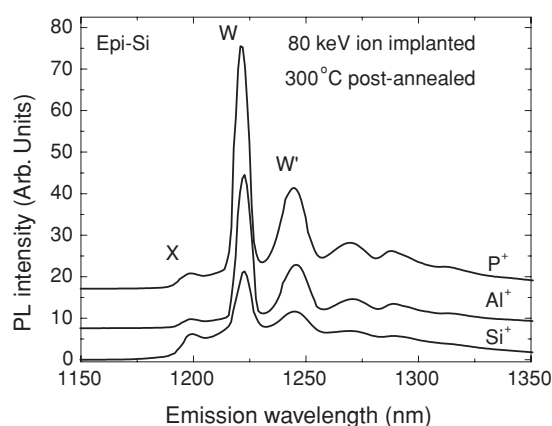


**Figure 1.** PL spectra of n-type epitaxial Si implanted with 80 keV  $\text{Si}^+$ ,  $\text{Al}^+$  and  $\text{P}^+$  ions and post-annealed at  $300^\circ\text{C}$  for 1 h. The spectra are shifted upwards vertically for clarity without changing the scaling. The principal peaks are denoted as X band (1200 nm), W band (1218 nm) and W' band (1245 nm). W-band intensity is highest with  $\text{P}^+$ -ion implantation.

understood in the framework of the stability of the I-clusters as they evolve from compact to elongated defect structures.

## 2. Experimental details

The experiments were performed on epitaxially grown and CZ grown (high content of oxygen and carbon impurity) n-type and p-type silicon wafers. Epitaxial n-Si samples were implanted at room temperature with 80 keV  $\text{Al}^+$ ,  $\text{Si}^+$  and  $\text{P}^+$  ions at a dose of  $1 \times 10^{14} \text{ cm}^{-2}$ . CZ-grown n-type and p-type silicon samples were implanted with 145 keV and 1.2 MeV  $\text{Si}^+$  ions in the dose range  $1 \times 10^{12}$  to  $5 \times 10^{13} \text{ cm}^{-2}$ . Post-implantation annealing was performed under  $\text{N}_2$  ambient in the temperature range of  $150$ – $750^\circ\text{C}$  for duration 30 min to 4 h. PL measurements were performed at 17 K and the luminescence was excited using Ar laser tuned to 488 nm. The luminescence was analysed using a CVI spectrometer with a single grating monochromator, and a liquid-nitrogen cooled Ge diode detector was used with a lock-in technique to record the signal. Temperature quenching of the PL was measured at the peak emission wavelength with a temperature scan from 17 K to 100 K. Depth profile of the luminescent centres was studied by step-by-step removal of the top Si layer by standard sputter etching technique.

## 3. Results and discussion

### 3.1. Low temperature annealing (up to $450^\circ\text{C}$ )

PL measurements on as-implanted and annealed samples show a well-known W band at 1218 nm, and the intensity of this peak achieves maximum upon annealing at  $300^\circ\text{C}$  [22]. Figure 1 shows a set of PL spectra for the epitaxial Si wafers implanted with different ion species (Si, Al and P) and post-annealed at  $300^\circ\text{C}$  for 1 h. The intense W band at 1218 nm corresponds to a small I-cluster in silicon, as is found at a depth much larger than the ion range [22] and the occurrence of W-band PL is independent of implant ion species. The W' band at 1244 nm is a phonon replica of the W band. The peak X at 1200 nm

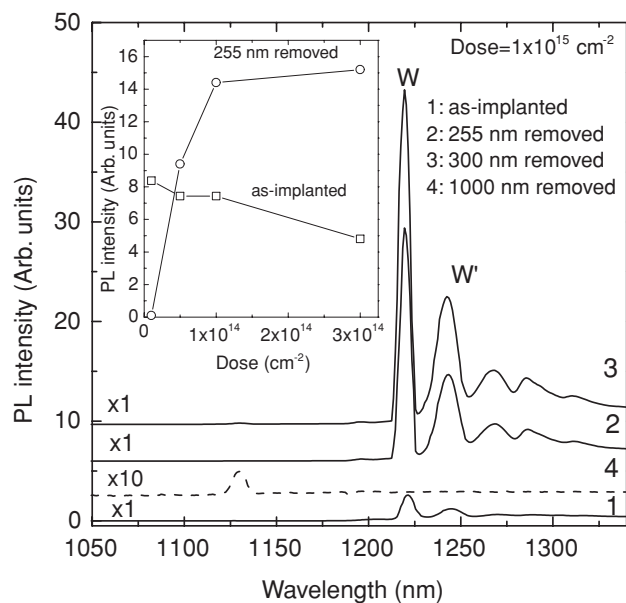


**Figure 2.** PL spectra of 80 keV Si<sup>+</sup> implanted at 260 °C on Si with a dose of  $1 \times 10^{15} \text{ cm}^{-2}$ : (1) as-implanted Si layer, (2) after removal of top 255 nm of Si layer (ion damaged), (3) 300 nm removed, (4) 1000 nm removed. Inset shows the dose dependence of PL intensity in as-implanted and 255 nm removed Si layer. W-band intensity attains the highest value after the removal of the top 300 nm of the Si layer.

has also been reported earlier [23] and it is believed to originate from a bigger I-cluster, as the X band grows at the cost of the W band at temperatures above 300 °C [24]. We studied the PL intensity of the W band as a function of Si-ion dose. In the as-implanted Si, W-band intensity is found to decrease with the dose in the range  $1 \times 10^{13}$  to  $3 \times 10^{14} \text{ cm}^{-2}$ , as shown in the inset of figure 2. To isolate the location of the corresponding radiative and nonradiative centres, we have performed the PL measurements at various depths of the implanted samples by controlled removal of the top Si layers. Figure 2 shows the PL spectra of the as-implanted Si layer and after the removal of the top 255 nm, 300 nm and 1000 nm Si layers from the same implanted sample. The W-band intensity clearly increases with the removal of the layer that is directly damaged by implanted ions or the vacancy rich layer. SRIM [25] calculation, a Monte Carlo code, of the damage profile using 80 keV Si ions show that the damaged region extends up to a maximum depth of  $\sim 200$  nm. We found that W-band defects are formed at a depth of  $\sim 300$  nm. Our results clearly show that the W centre is formed as a result of migrating defects species and these defects must form stable I-clusters, even at room temperature and with the smallest ion dose. Hence, the responsible defect should be one of the smallest clusters that form upon irradiation. When the implantation is performed at elevated temperature where the W-band intensity becomes highest, we found that the X-band intensity does not change appreciably though the W-band intensity increases many folds upon the removal of the top silicon layer. For 300 °C annealing, the W-line intensity attains a maximum, and at 450 °C the X-band intensity grows whereas the W-band intensity diminishes and becomes comparable to the intensity of the W band. This implies that the X band is developed at the cost of the W band, and the X band arises due to the formation of bigger

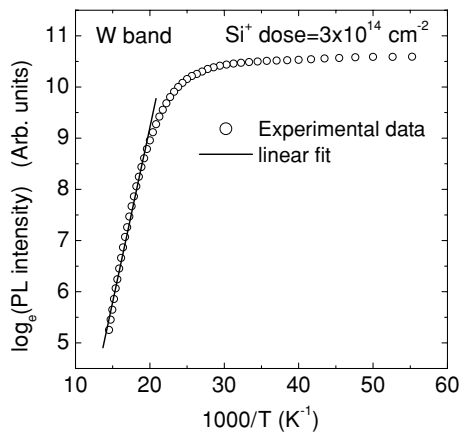


**Figure 3.** W-band intensity as a function of inverse temperature measured in the range of 17–100 K. The slope of the fitted line is used to determine the deactivation energy for the PL quenching.

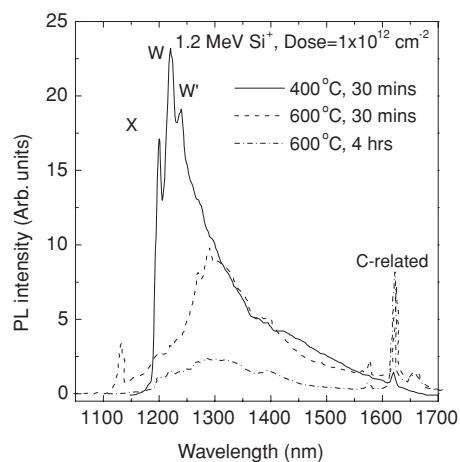


**Figure 4.** PL spectra of p-type CZ Si implanted with 1.2 MeV Si<sup>+</sup> ions to a dose of  $1 \times 10^{12} \text{ cm}^{-2}$  and annealed at various temperatures. The peak at 1619 nm (C-related) is due to an interstitial carbon related centre.

I-clusters which must be derived from the W-band-related I-clusters. We believe that this is a key point to the understanding of the structure of the W-band-related defect. The W-band PL intensity is found to be very intense in annealed silicon or silicon implanted at elevated temperature. We measured the PL intensity of the W band at the peak wavelength (1218 nm) at various temperatures under a slow scan of temperature. However, the PL intensity drastically reduces above  $\sim 50$  K as shown in figure 3. We calculated a deactivation energy of 59 meV for the thermal quenching of the W band using an exponential relationship. This energy is close to the energy of the spectroscopic displacement energy of the defect from the band edge suggesting a bound-to-free thermal activation for the W band. This low temperature quenching of the W band implies that the corresponding defect is not favourable for exploiting the room temperature light emission from Si.

### 3.2. Intermediate temperature annealing (600 °C)

Annealing at 600 °C shows a drastic change in the PL spectra for all the implanted samples as shown in figure 4. A high

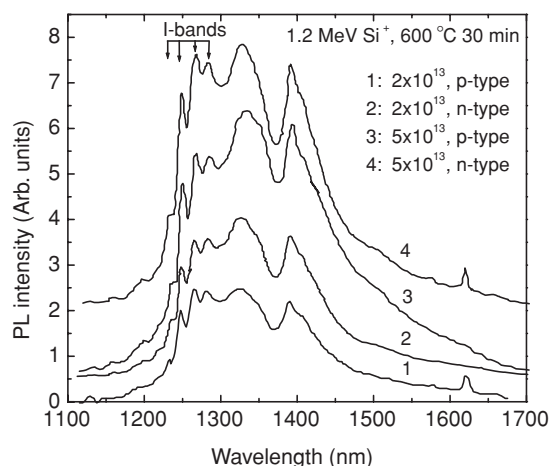


**Figure 5.** PL spectra of 600 °C for 30 min annealed p-type and n-type Si implanted with two different doses. Sharp PL peaks (I bands shown with arrows) on the broad envelope in the range of 1228–1400 nm are characteristics of I-clusters formed with high energy and high dose ion implantation. Individual curves are shifted vertically upwards for clarity of presentation.

energy (MeV) low dose ( $1 \times 10^{12} \text{ cm}^{-2}$ )  $\text{Si}^+$  implanted sample shows a relatively broad peak with two small peaks (at  $\sim 1269 \text{ nm}$  and  $\sim 1290 \text{ nm}$ ) overlapping on it. These small peaks disappear for longer duration annealing (see figure 4), indicating the possible dissolution of the defect complexes. These small peaks may be related to the formation of some I-clusters that do not emit light efficiently. Note that low energy (keV) high dose  $\text{Al}^+$  or  $\text{P}^+$  implantation showed similar broad PL peaks centred at  $\sim 1340 \text{ nm}$  after 600 °C annealing [26]. On the other hand, when Si ions are implanted at MeV energy and high dose ( $\geq 10^{13} \text{ cm}^{-2}$ ), both the n-type and p-type Si samples exhibit several sharp PL peaks in the wavelength range of 1228–1400 nm (labelled as I bands) after annealing at 600 °C for 30 min, as shown in figure 5. The intensity of these I bands (at 1227 nm, 1240 nm, 1260 nm and 1275 nm, shown with arrows) does not change appreciably with dose, and they seem to be lying over a broad envelope (peak) whose intensity increases with dose. The I-band features are exactly identical for n-type and p-type Si. Similar features have been reported earlier [4, 5, 21], but no satisfactory explanation exists for the multiplicity of peak structures. In order to better understand the nature of defects involved for the PL peaks, we studied the influence of  $\text{Si}^+$  ion energy keeping the ion dose and post-implantation processing conditions unchanged. The effect is shown in figure 6 for a dose of  $2 \times 10^{13} \text{ cm}^{-2}$ . The data are scaled appropriately to enable comparison; the keV implanted sample, in fact, shows a lower intensity of PL. It is evident from the spectra that when compared with MeV implantation, keV ions do not induce these multiple sharp peaks; instead only two broad peaks centred at  $\sim 1300 \text{ nm}$  and  $\sim 1392 \text{ nm}$  are observed. Note that the peak at  $\sim 1392 \text{ nm}$  is common to both cases. Hence, the multiple PL peaks in MeV implanted samples may originate from a complex I-cluster or large I-cluster possessing multiple configurations. These defects form due to supersaturation of Si interstitials resulting from the high energy impact of the ions into Si. This is a key result for understanding the origin of the I bands that appear for the intermediate temperature of annealing. When these samples,

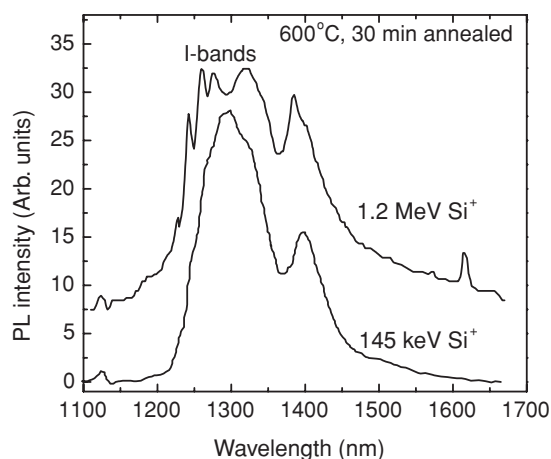


**Figure 6.** Comparison of the PL spectra for different implantation energy: 1.2 MeV and 145 keV  $\text{Si}^+$  ions implanted on Si and post-annealed at 600 °C for 30 min. No I bands are detected in keV implanted Si.

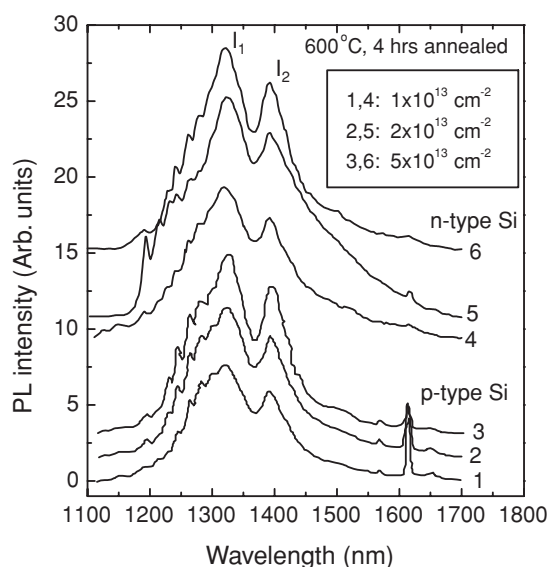


**Figure 7.** PL spectra of MeV  $\text{Si}^+$  implanted on Si at various doses and post-annealed at 600 °C for 4 h. The spectra are shown for three different doses on both n-type and p-type CZ Si. Two major peaks are labelled as  $I_1$  (1322 nm) and  $I_2$  (1394 nm) bands in these sets of spectra.

exhibiting multiple PL peaks, are further annealed for 4 h at 600 °C two broad peaks at  $\sim 1322 \text{ nm}$  ( $I_1$ ) and  $\sim 1392 \text{ nm}$  ( $I_2$ ) survive. This feature is exactly identical in both p-type and n-type Si as shown in figure 7, where the spectra are shown for three different doses. Note that the line widths of the peaks  $I_1$  and  $I_2$  are quite large as compared to those of the W and X bands discussed in the previous section. Whereas the X and W bands showed a full width at half maximum (FWHM) of only  $\sim 7\text{--}8 \text{ meV}$ , we estimated a FWHM of  $\sim 80 \text{ meV}$  for the  $I_1$  and  $I_2$  bands. Hence, the large FWHM of  $I_1$  and  $I_2$  bands indicates that the related defects have spread in activation energy and are likely to have an extended structure. These spectral features remain unchanged even for very long duration (up to 30 h) annealing, indicating the enhanced thermal stability of the relevant defects.

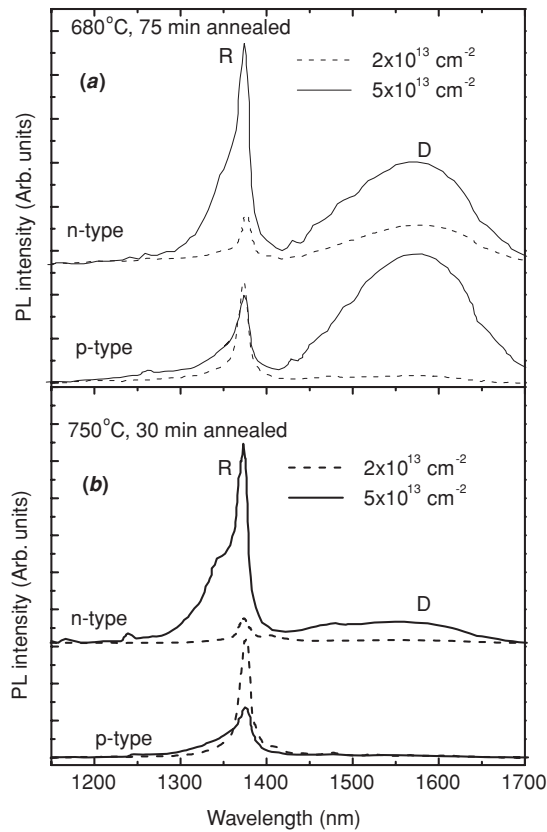


**Figure 8.** (a) PL spectra of MeV Si<sup>+</sup> implanted Si annealed at 680 °C for 75 min. The results are shown for two different doses and dopants (n-type and p-type) in Si. (b) PL spectra of similar samples annealed at 750 °C for 30 min. The sharp peak at 1376 nm is labelled as the R band and broad peak centred at ~1580 nm is labelled as the D band.

### 3.3. High temperature annealing ( $\geq 680$ °C)

When the annealing temperature is increased to 680 °C, the PL spectra are dramatically modified for the annealed samples. The PL spectra for n-type and p-type samples for two different doses are shown in figure 8(a) for annealing at 680 °C for 75 min. The spectra are dominated by a peak at 1376 nm (R band). With increasing dose, the R-band intensity increases with the appearance of another broad peak centred at ~1576 nm (D band). The effect of increasing the dose is also the broadening of the R band with a possible peak contributing at the higher energy side. This is particularly evident for the n-type sample. The R-band intensity further grows with annealing at higher temperatures. Figure 8(b) shows the result of 750 °C for 30 min annealing for the same two doses and different doping types. In this case the D-band intensity is found to be lower than that found for annealing at 680 °C. In particular, the 750 °C annealed p-type sample shows no D band, whereas the 680 °C annealed samples show comparable intensity of the R band and D band. Hence, the D band can be attributed to the radiative recombination at the residual damage or strained region formed by ion implantation. The 1376 nm peak has been previously observed by other groups [4, 5, 27] and has been directly correlated with the presence of rod-like  $\{3\ 1\ 1\}$  defects as observed by transmission electron microscopy [27]. Note that no R band was detected in the

samples implanted below a threshold dose of  $1 \times 10^{13}$  cm<sup>-2</sup> and annealing temperature below 680 °C. The complete transformation of the PL spectra after 680 °C from those of the 600 °C annealed samples and the presence of a threshold dose and annealing temperature indicates that a severe structural transformation may take place to form the R-band-related defects from the I-band defects [27]. The presence of lattice damage in the 680 °C annealed samples as evidenced by the broad D band implies that residual damage is present for 600 °C samples for all doses of  $\geq 1 \times 10^{13}$  cm<sup>-2</sup>. Hence, the broadening of the I<sub>1</sub> and I<sub>2</sub> bands in figure 7 is partly contributed by the lattice damage surrounding these defects. However, sharp I bands are characteristics of the bigger and stable I-clusters.

### 3.4. Classification and origin of the defects

The results presented in the previous sections show that the PL spectra are distinctly different for three different temperature regions defined as low (RT to 450 °C), intermediate (600 °C) and high ( $\geq 680$  °C) temperatures. The defect peaks observed in the present study can be classified into two groups according to their line shape: the sharp peaks (the W, X, R and I bands), and the broad peaks (the I<sub>1</sub>, I<sub>2</sub> and D bands). From our results and other reports [28], it is known that the W centre is a small I-cluster of Si. The number of interstitials in the W centre was estimated to be one or two by employing the law of mass action [28]. Since the X centre forms at a higher temperature than the formation of the W centre and accordingly is more stable than the latter, the number of interstitials in the X centre is thought to be larger than that of the W centre according to the concept of ripening of the clusters with the increase of annealing temperature [3]. In modelling the X centre, the tetragonal symmetry ( $D_{2d}$ ) and easy compressive nature of the centre [23] should be satisfied. Recently an ESR signature of the tetra-interstitial (I<sub>4</sub>) clusters in silicon has been obtained [18] that exactly correlates with the X-band PL and infrared absorption peaks at 530 and 550 cm<sup>-1</sup>. Hence, the X centre can be assigned to an I<sub>4</sub>-cluster. PL measurements show that the X centre is formed at the expense of the W centre, but the X centre formation is not simultaneous with the formation of the W centre even at elevated temperatures. This implies that the X centre does not form as a result of simple addition of mono-interstitials to the W centre as would be expected from the simplest way of cluster ripening. Instead, the X-centre defect must evolve from a possible combination of the W centre defects. This is a key point for building a model structure for the W centre. Hence, the W centre may consist of a half unit of the X centre or I<sub>4</sub>-cluster. Accordingly, the I<sub>2</sub>-cluster is the most likely candidate for the W centre, which can easily combine to form an I<sub>4</sub>-cluster upon the supply of thermal energy. The possibility of an I<sub>3</sub>-cluster being responsible for the W band has been ruled out recently [12, 28]. The extremely mobile model of I<sub>3</sub> [11] does not corroborate with our observation that the defect was not found at a depth of 1.0 μm, and the defect is formed by low mass ions or electrons even at room temperature. Nakamura *et al* [28] argued on the basis of symmetry requirement and formation order of the W centre that  $\langle 1\ 1\ 1 \rangle$  split monointerstitial or the  $\langle 1\ 1\ 1 \rangle$  ST di-interstitial are the most probable defects responsible for the

W-band PL. However, the monointerstitial model is unlikely to survive at elevated temperature and they are expected to form at a very large depth due to their extremely mobile nature. The ST di-interstitial model is synthesized from a  $\langle 110 \rangle$  split interstitial and a T interstitial and consists of three silicon atoms sharing one lattice site and forming an equilateral triangle in a  $\langle 111 \rangle$  plane. The +2 charge state of the  $\langle 111 \rangle$  ST di-interstitial is the most stable (the formation enthalpy is 3.0 eV) among several charge states of three di-interstitials calculated in [28]. In our view, the  $\langle 111 \rangle$  ST di-interstitial model is more appropriate for the W centre, as this has the required symmetry and can easily transform to an  $I_4$  structure by the aggregation of two di-interstitials upon annealing. This  $I_4$  structure is known to be responsible for the X-band PL [17]. Hence, we assign the W-band PL to the  $\langle 111 \rangle$  ST di-interstitial defect and the X-band PL to the  $I_4$  defect. As the defect is formed in the undamaged region of the crystal and we observe a sharp PL line shape for the W band irrespective of the ion dose, this is clearly indicative of the small and compact shape of the clusters with a well-defined energy level in the band gap of Si.

In the case of the W and X bands, we observe a FWHM of only  $\sim 6\text{--}7$  meV which is close to that found for the TO phonon line observed for excitonic recombination. Note that in the PL measurements we used a scan step of 1 nm for all spectra acquired and this is the smallest line width observed for the recombination at a point defect. Hence, we classify the W and X bands as arising from the compact small I-clusters with  $I_2$  and  $I_4$  structures, respectively. Similar sharp features are observed for some of the I bands shown in figure 5. However, the major change in the PL spectra after 600 °C annealing indicates the corresponding change in the structure and configuration of the I-clusters. In the literature, a similar PL signature has been attributed to the precursor of  $\{311\}$  defects [29]. However, Nakamura *et al* [21] did not support this assignment, as they did not observe the evolution of  $\{311\}$  defects even when the multiple peaks or broad peaks were observed. Libertino *et al* [5] attributed similar peaks to I-clusters, without proposing any specific structure. Cowern *et al* [19] suggested that during the first few minutes of annealing at 600 °C, the majority of the clusters remain with size  $n = 8$ , for longer duration annealing nearly half of the clustered interstitials remain of size 8 and half of the clusters have a size distribution in the range  $n = 10\text{--}100$ . As discussed above, the majority of the I-clusters remain of the size  $n = 4$  for annealing up to 450 °C, and these  $I_4$ -clusters grow further to an  $I_8$  structure in the initial stages of annealing at 600 °C. However, a number (at least four) of sharp peaks present in the I bands cannot be explained by assuming the presence of  $I_8$ -clusters alone. On the other hand, a broad distribution of clusters with sizes in the range of 10–100 cannot account for these few peaks with relatively sharp features. Figure 8 shows that the 600 °C annealed sample contains residual lattice damage that can account for the broad envelope over which the relatively sharp I bands are superposed. Theoretical predictions show that several configurations of an I-cluster can have almost the same stability energy and correspondingly, in the present study these I bands could be the manifestation of the multiple configurations of the  $I_8$ -clusters. In the literature, even smaller I-clusters such as  $I_3$  and  $I_4$  are proposed to have

possible multiple configurations [11–13]. Therefore these I bands are likely to originate from metastable configurations of compact but bigger I-clusters such as  $I_4$  and  $I_8$ . However, none of the explicit numbers in these bigger clusters has been estimated yet and structure determination of the centres remains an open question. Electrical signature of metastability [30] of I-clusters in Si has been provided from capacitance transient spectroscopic studies. However, no direct correlation exists in the literature with the optical studies. Another possible mechanism for the multiple PL peaks is the transition from different excited states to the same ground state of a large I-cluster. For example, NL51 ESR spectra of electron irradiated Si have been attributed to an excited state of the neutral  $I_4$  defect [31], while the positive charge state of the  $I_4$  defect has been correlated with the B3-ESR spectra [18]. Luminescence excitation spectra of diamond show a series of similar undocumented PL peaks that were thought to be due to radiative transitions from different excited states to the same ground state of a divacancy-related centre [32]. Similar mechanism may be operative in the occurrence of the multiple PL peaks in the present study. However, more studies would be required to pinpoint a specific mechanism.

When the 600 °C annealing is performed for a longer duration (4 h to 30 h) the two broad bands  $I_1$  and  $I_2$  appear in all the samples irrespective of the ion dose and doping type. These broad peaks have a FWHM of about  $\sim 75$  meV, which is quite large compared to that of the W and X bands. We attribute this line shape broadening to the presence of lattice strain and the extended structure of the corresponding I-clusters. Impurity precipitates in silicon show a similarly broadened PL spectrum with a FWHM of  $\sim 50$  meV or more depending on the amount of strain involved in the lattice [33]. Strain-induced quantum confinement of the carrier has been proposed to account for the broad PL bands corresponding to a change in the local band gap [34]. Weman *et al* [34] proposed that a compressive strain field around an extended defect reducing the lattice constant by about 3% is sufficient to reduce the band gap locally by as much as 0.3 eV. In the present case, the positions of the two peaks  $I_1$  and  $I_2$  would correspond to a lattice-strain of about 2%.

In the model simulations, classification of the interstitial defects provided by Kim *et al* [10] is useful. According to them, the stable defect configurations evolve from a compact to a chain-like to a rod-like  $\{311\}$  defect with an increasing number of interstitials. When the  $\langle 111 \rangle$  split interstitial model is used as the building unit for the bigger clusters, the compact clusters are more stable than the chainlike clusters up to four interstitials, and there is a discontinuity in the formation energy between the compact and chainlike configurations [10]. With the help of high resolution transmission electron microscopy, Schmidt *et al* have identified nanometer sized clusters [4] in Si implanted (dose =  $1 \times 10^{14}$  cm $^{-2}$ ) Si annealed at 525 °C. This was a rather direct verification of the predictions made by Kim *et al*. It is well known that the PL spectral line shape is a characteristic of the strain in the defect/lattice. DLTS studies on similarly treated samples have shown energy broadening up to  $\sim 30$  meV for the related I-clusters [5]. Hence, we attribute the broad  $I_1$  and  $I_2$  bands to the I-chains that form upon annealing at 600 °C. Nakamura *et al* [21] have argued that these defects do not directly evolve to  $\{311\}$  rod-like defects as they do not detect the R band in copper and proton implanted

Si after 750 °C annealing. This is consistent with the proposal made by Coffa *et al* [27]. For annealing at 680 °C and Si ion dose of  $\geq 1 \times 10^{13} \text{ cm}^{-2}$ , the 1376 nm R band detected in our studies as well as other studies corroborates with the presence of {3 1 1} rod-like defects. Hence, the R band results from the recombination of carriers at these defects. The line shape analysis for the R band shows a FWHM of  $\sim 10 \text{ meV}$ , which is of the same order as found for the W and X bands. Hence, the formation of the {3 1 1} defects involves the release of strain from the I-chains or extended I-clusters. As these defects give rise to a well-defined energy level in the forbidden gap of Si, the corresponding PL peak is sharp. This is analogous to the occurrence of D-band PL lines in dislocated Si. Dislocation-related D bands [35] in Si have similarly sharp line widths and correspond to well-defined energy levels as determined electrically.

#### 4. Conclusions

Low temperature photoluminescence studies in ion-implanted Si show the distinct signature of self-interstitial clusters of various sizes. Small and compact I-clusters are characterized by sharp PL peaks at 1200 nm and 1218 nm, irrespective of ion species, dose and energy. We have argued that while the 1200 nm peak is due to a tetra-interstitial ( $I_4$ ) cluster, the 1218 nm peak is ascribed to a ST di-interstitial ( $I_2$ ) cluster. For high energy self-ion implanted Si, short duration annealing at 600 °C induces a number of PL peaks in the range of 1228–1400 nm that are ascribed to bigger I-clusters, such as  $I_8$ , possessing multiple configurations and/or allows excited state transitions. Prolonged annealing at 600 °C induces  $\langle 110 \rangle$  oriented chains of I-clusters that give rise to two broad PL peaks centred at 1322 and 1392 nm. Finally, for a dose of  $\geq 1 \times 10^{13} \text{ cm}^{-2}$  and an annealing temperature  $\geq 680 \text{ °C}$ , a sharp and intense PL band at 1376 nm is observed for both n-type and p-type Si, which is attributed to the recombination at {3 1 1} rod-like defects. The changing line-width of the PL spectra after different stages of annealing is believed to result from the shape evolution of the I-clusters from compact to extended structures. These results corroborate the recent theoretical predictions about the trends in the growth of extended interstitial defects in Si.

#### Acknowledgments

This work was partly supported by the financial aid from ICTP, Trieste. We are thankful to S Coffa and E Rimini for their help in the photoluminescence measurements.

#### References

- [1] See, e.g., Stolk P A, Gossmann H-J, Eaglesham D J, Jacobson D C, Rafferty C S, Gilmer G H, Jaraíz M, Poate J M,

- Luftman H S and Haynes T E 1997 *J. Appl. Phys.* **81** 6031, and references therein
- [2] Kohyama M and Takeda S 1992 *Phys. Rev. B* **46** 12305
- [3] Benton J L, Halliburton K, Libertino S, Eaglesham D J and Coffa S 1998 *J. Appl. Phys.* **84** 4749
- [4] Schmidt D C, Svensson B G, Seibt M, Jagadish C and Davies G 2000 *J. Appl. Phys.* **88** 2309
- [5] Libertino S, Coffa S and Benton J L 2001 *Phys. Rev. B* **63** 195206
- [6] Takeda S, Kohyama M and Ibe K 1994 *Phil. Mag. A* **70** 287
- [7] Aria N, Takeda S and Kohyama M 1997 *Phys. Rev. Lett.* **78** 4265
- [8] Tang M, Colombo L, Zhu J and Rubia T D 1997 *Phys. Rev. B* **55** 14279
- [9] Coomer B J, Goss J P, Jones R, Oberg S and Briddon P R 1999 *Physica B* **273–274** 505
- [10] Kim J, Kirchoff F, Wilkins J W and Khan F S 2000 *Phys. Rev. Lett.* **84** 503
- [11] Estreicher S K, Gharaibeh M, Fedders P A and Ordejon P 2001 *Phys. Rev. Lett.* **86** 1247, and references therein
- [12] Lopez G M and Fiorentine V 2004 *Phys. Rev. B* **69** 155206
- [13] Richi D A, Kim J, Barr S A, Hazzard K R A, Hennig R and Wilkins J W 2004 *Phys. Rev. Lett.* **92** 045501
- [14] Blumenau A T, Jones R, Oberg S, Briddon P R and Fruenheim P 2001 *Phys. Rev. Lett.* **87** 187404
- [15] Kirkpatrick C G, Myers D R and Streetman B G 1976 *Radiat. Eff.* **30** 97
- [16] Lopez G M and Fiorentini V 2003 *J. Phys.: Condens. Matter* **15** 7851
- [17] Coomer B J, Goss J P, Jones R, Oberg S and Broddon P R 2001 *J. Phys.: Condens. Matter* **13** L1
- [18] Mechedlidze T and Suezawa M 2003 *J. Phys.: Condens. Matter* **15** 3683
- [19] Cowern N E B, Mannino G, Stolk P A, Roozeboom F, Huizing H G A, van Berkum G J M, Christiano F, Claveri A and Jaraíz M 1999 *Phys. Rev. Lett.* **82** 4460
- [20] Schiettekatte F, Roorda S, Poirier R, Fortin M O, Chazal S and Heliou R 2000 *Appl. Phys. Lett.* **77** 4322
- [21] Nakamura M and Murakami S 2003 *J. Appl. Phys.* **94** 3075
- [22] Giri P K, Coffa S and Rimini E 2001 *Appl. Phys. Lett.* **78** 291
- [23] Ciechanowska Z, Davies G and Lightowers E C 1984 *Solid State Commun.* **49** 427
- [24] Harding R, Davies G, Coleman P G, Burrows C P and Wong-Leung J 2003 *Physica B* **340–342** 738
- [25] <http://www.srim.org/SRIM/SRIM2003.htm>
- [26] Giri P K 2003 *Physica B* **340–342** 734
- [27] Coffa S, Libertino S and Spinella C 2000 *Appl. Phys. Lett.* **76** 321
- [28] Nakamura M and Nagai S 2002 *Phys. Rev. B* **66** 155204
- [29] Tsuji H, Kim R, Hirose T, Shano T, Kamakura Y and Taniguchi K 2002 *Mater. Sci. Eng. B* **91** 43
- [30] Giri P K 2003 *Physica B* **340–342** 729
- [31] Mechedlidze T, Yonenaga I and Suezawa M 2003 *Mater. Sci. Semicond. Process.* **6** 263
- [32] Ikoubovskii K and Adriaenssens G J 2000 *Phys. Rev. B* **61** 10174
- [33] Giri P K, Coffa S, Raineri V, Privetera V, Galvagno G, La Ferla A and Rimini E 2001 *J. Appl. Phys.* **89** 4310
- [34] Weman H, Monemar B, Oehrleim G S and Jeng S J 1990 *Phys. Rev. B* **42** 3109
- [35] Sauer R, Weber J, Stolz J, Weber E R, Kusters K-H and Alexander H 1985 *Appl. Phys. A* **36** 1